

Late Arriving Particles in Cosmic Ray Air Showers and AGASA's Determination of UHECR Energies

Hans-Joachim Drescher^{1,2} and Glennys R. Farrar¹

(1) *Center for Cosmology and Particle Physics,
Department of Physics, New York University,
4 Washington Place, New York, NY 10003*

(2) *Frankfurt Institute for Advanced Studies
Johann Wolfgang Goethe-Universität
Max-von-Laue Str. 1,
60438 Frankfurt am Main, Germany*

We give the first detailed study of the arrival time distribution of nucleons in UHECR air showers. We analyze in detail the influence of late arriving particles on the energy determination of the AGASA experiment, as well as how the arrival time distribution changes with distance from shower core. Our calculations are consistent with experimental observations of the AGASA group. Crucial to obtaining agreement, is the correct implementation of the energy loss for low-energy protons. We confirm AGASA's estimation of the error in their energy determination associated with late-arriving particles, assuming primary protons.

I. INTRODUCTION

The results of the AGASA collaboration have been followed with great interest throughout the years because they had the largest exposure for highest energy cosmic rays. As of now, AGASA reports about 10 cosmic ray events with an energy greater than 10^{20} eV[1], well beyond the predicted GZK cutoff due to interaction of particles with the cosmic microwave background, assuming uniformly distributed sources. By contrast, the HiRes collaboration reports that their monocular results are consistent with a GZK cutoff[2]. The statistics are not yet sufficient to decide whether this is a significant discrepancy or not, but the question of whether there is a systematic shift between the relative energy normalizations of AGASA and HiRes has assumed special importance. AGASA is an extensive air shower array detector while HiRes uses the air fluorescence technique.

In this paper we investigate the contribution of nucleons to AGASA's energy determination, which has been neglected in previous analyses. The energy determination in AGASA is based on the particle density, measured with plastic scintillator detectors. The reconstructed value of the signal at a distance of 600m from the core is used as an energy estimator, since this is considered to be rather insensitive to fluctuations and to not depend too much on the air shower model. The density of nucleons at 600m is not negligible. Neutrons (unlike protons) have a small energy deposit in plastic scintillator but they scatter elastically with protons in the scintillator. The arrival-time-delay distribution of neutrons is very broad and, due to AGASA's technique for recording the signal, late arriving particles have an exponentially increased weight as is explained below. This is the motivation for our scrutiny of the issue of late arriving particles in general and nucleons in particular. HiRes' energy measurement entails an entirely different set of issues and

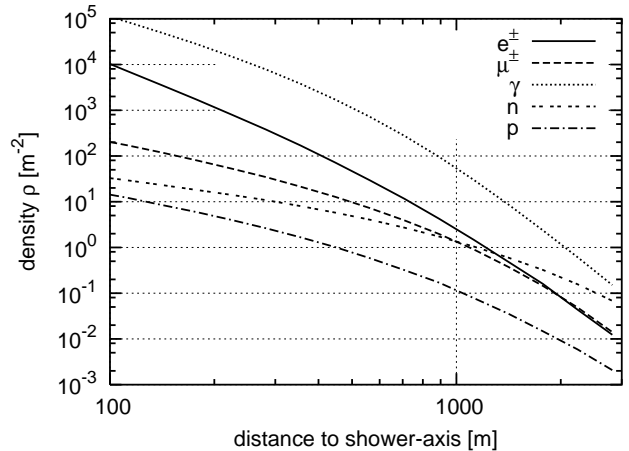


FIG. 1: Lateral distribution of particle density as a function of distance from the core in a 1×10^{19} eV proton-induced shower.

systematic uncertainties which we do not address in this paper.

II. GROUND NUCLEONS

The air-showers analyzed in this paper are simulated with the SENECA model, as introduced in [3]. The basic features of this model are the high energy hadronic model QGSJET01 [4], the electro-magnetic shower model EGS4 [5], and different choices of the low-energy hadronic model: GHEISHA [6], which was the default option in the CORSIKA model, G-FLUKA [7] and GCALOR [8] used in the framework of the GEANT 3.21[8, 9] package for detector simulation. The model also has some new simulation techniques which speed up the computation of air showers considerably, by using the approach of

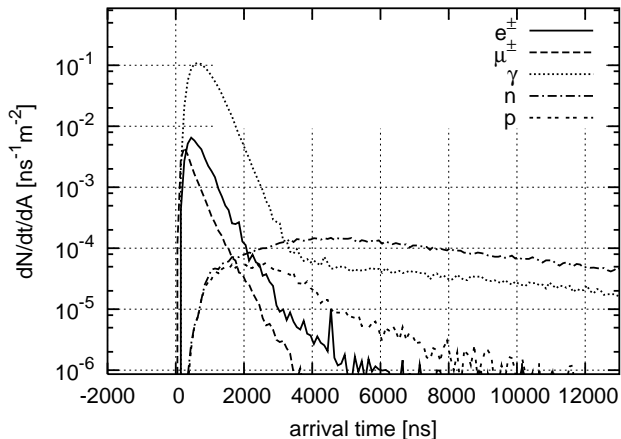


FIG. 2: Arrival time distribution for particles at 600 m from the shower-core. Times are with respect to the arrival of the shower-core.

cascade equations as described in detail in ref. [10]. The pure physics content (hadronic and electromagnetic modelling) using GHEISHA as low-energy hadronic model, is identical to the one of CORSIKA [11], and the results are in good agreement with this model.

Figure 1 shows the averaged lateral distribution of particle densities as a function of the distance from the shower core, generated by 1×10^{19} eV vertical proton showers at an altitude 667m above sea level, using GCALOR as the low-energy hadronic model. All particles have been plotted which have kinetic energies ≥ 1 MeV. Neutrons become quite prominent at large distances from the shower-core, unlike protons which are more readily absorbed in the atmosphere due to ionization energy loss.

Electromagnetic particles and muons arrive within about a micro-second, whereas nucleons can be retarded by many tens of microseconds due to multiple scatterings. The arrival time distribution of particles of various species, 600 m from the core, is shown in Fig. 2. Arrival times are measured with respect to the arrival of the shower core.

III. PARTICLE MEASUREMENT IN AGASA

A particle of a specified type, kinetic energy and incidence angle, gives a certain energy deposit in AGASA's 5 cm thick plastic scintillator. When a charged particle passes through the detector, the signal from the photons generated in the scintillator and detected by the photomultiplier is processed to produce a signal which decays exponentially, with a time constant of $10\mu s$. The time duration in which the signal has an amplitude greater than a given discrimination level is called the pulse-width. Recording the pulse-width rather than the signal itself has the advantage that a large dynamic range of energy

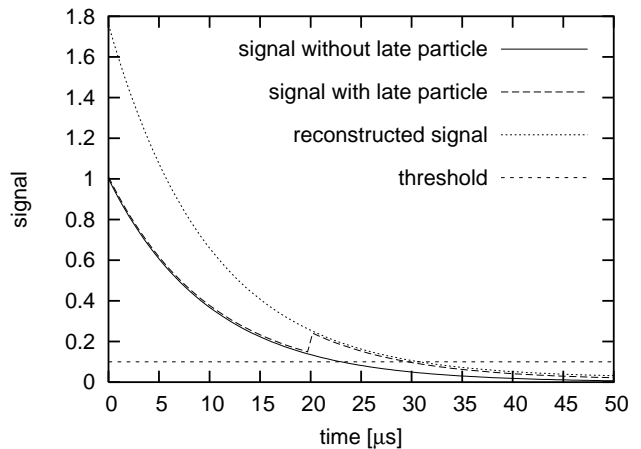


FIG. 3: How late arriving particles depositing 10% of the initial energy deposit can fake a signal 1.7 times higher.

deposit is measurable, since the pulse-width is proportional to the logarithm of the energy deposit.

An important assumption is that all particles arrive in a time much shorter than the decay constant of the signal. The bulk of particles arrive in less than a micro-second, but neutrons can scatter for a much longer time since they do not lose energy by ionization of air molecules, as is reflected in Fig. 2. The effect of a particle arriving $20\mu s$ late, with an energy deposit 10% as large as the original signal, is shown in Fig. 3. Even though the late energy deposit in this particular example is small, the time delay increases its importance by a factor of $\exp(20\mu s/10\mu s) = 7.4$ and the inferred total energy deposit is overestimated by roughly a factor of 1.7.

One can easily calculate the effect of this time delay for the measurement of particle densities. It increases the signal by the factor

$$f = \frac{\int_{t_0}^{t_1} \frac{dE_{\text{dep}}}{dt} \exp((t - t_0)/10\mu s) dt}{\int_{t_0}^{t_2} \frac{dE_{\text{dep}}}{dt} dt}, \quad (1)$$

where t_0 is the time when the detector triggered and t_1 is the time when the signal falls below the threshold or $128\mu s$, whichever is less. t_2 represents the arrival time of the last particle, not necessarily equal to t_1 . Thus f is the factor by which the measured signal has to be reduced in order to obtain the true energy deposit in a detector.

Figure 4 shows f as a function of radius for the total signal of electrons, muons and photons, using the shower simulation described in section II. The factor f increases as a function of the radius due to greater spreading of the arrival times at large distance. At very large distances f decreases again, when the particle number in a detector falls to of order unity. If a single particle arrives at a detector, $f = 1$ as is evident from replacing dE_{dep}/dt in eq. (1) with a delta function at t_0 . However f can also be less than 1, since in general the arrival time t_2 can be larger than the time t_1 when the pulse falls below the

threshold. If for example a second particles arrives after t_1 the AGASA acquisition system generates a second signal but it is ignored in the analysis. Effects arising when the particle number is of order one are a function of the area of the detector and primary energy as well as distance to the core. The AGASA collaboration measured the effect of the arrival time distribution, in a 30 m² detector with time-resolution as described in ref. [1].

IV. EFFECT OF NEUTRONS AND PROTONS IN A PLASTIC SCINTILLATOR

The energy-deposit of neutrons in a 5cm-plastic scintillator is calculated with the GEANT-package [9] and the Gcalor interface [8] relevant for low energy neutrons below 10 GeV. Above 10 GeV, routines from the FLUKA package are called automatically [7]. The geometrical setup consists of a 1.5m x 1.5m x 5cm plastic scintillator in a 1.6mm thick iron box which is placed in a farmer's storage house made with 0.4mm thick iron plates. We have checked that we can reproduce the energy deposit spectra used by the AGASA-collaboration for electrons, positrons, muons and photons [12]. Protons deposit energy in a plastic scintillator since they are charged particles. The main process is ionization. Neutrons affect the scintillator by scattering elastically with the protons of hydrogen abundantly available in plastic scintillators; the recoil protons then deposit energy [13].

The energy deposit spectra of neutrons and protons are shown in figure 5 for particles arriving at different angles. One sees the increasing energy deposit due to the longer path length in the material scaling with $1/\cos(\theta)$.

If the energy deposit in a scintillator is locally concentrated, a saturation of the scintillation response is observed. The impact of this on the scintillation signal generated by neutrons and protons is described by Birks' law [14], and is shown in Fig. 6. Throughout our calculations, the effect of Birks' law has been included, using the parameters proposed in the GEANT manual which are consistent with values proposed in [14]. The result is expressed by quoting an effective energy deposit, which would give the equivalent scintillator response in the absence of this effect.

V. CALIBRATION OF THE THEORY

AGASA calibrates their detectors with the ambient signal from atmospheric muons, also called "omnidirectional" muons, which are the dominant source of signals in individual detectors. Because these muons are close to being minimum-ionizing, the energy deposited by a single muon depends primarily on its angle (tracklength) and depends only weakly on its energy. Therefore the pulsewidth distribution of an individual detector is well understood and suitable for calibrating the scintillator response. We calibrate the theory in the same way.

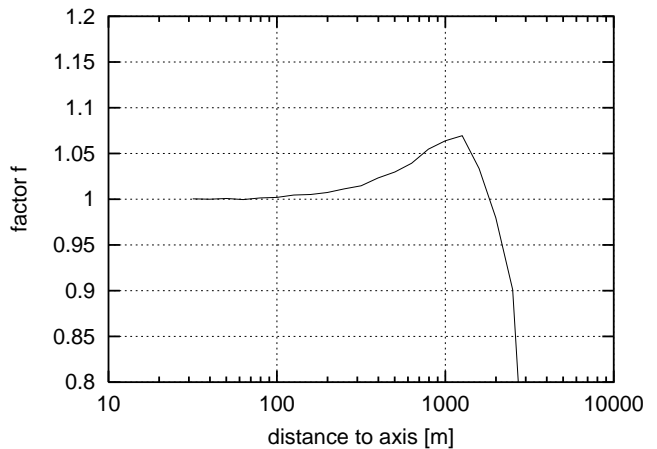


FIG. 4: The effect of time delay on the measurement of the total energy deposit of electrons, muons and photons.

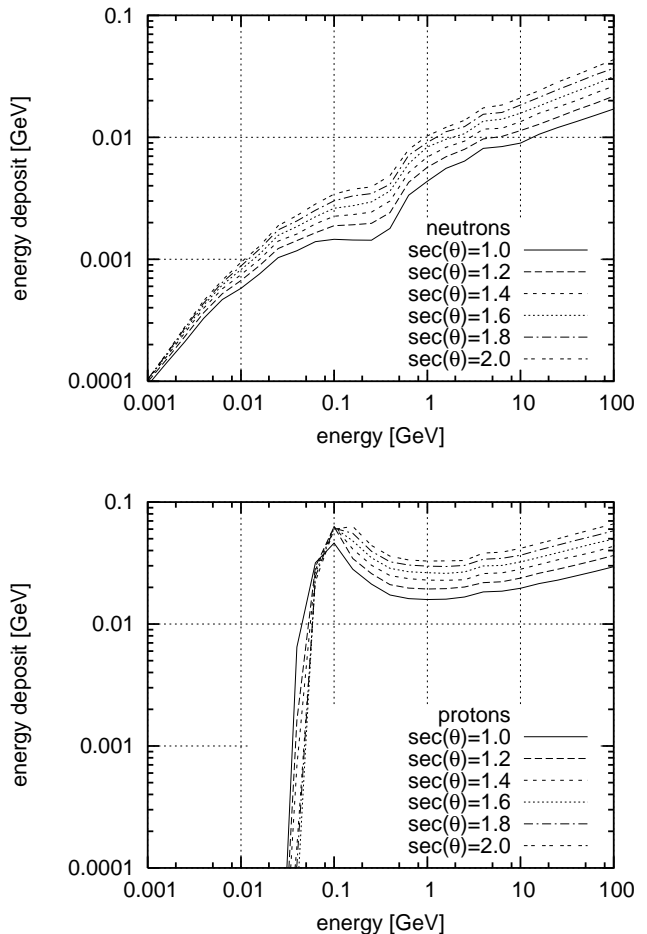


FIG. 5: Energy deposit in a 5cm plastic scintillator of vertically arriving neutrons (top) and protons (bottom) of different energies.

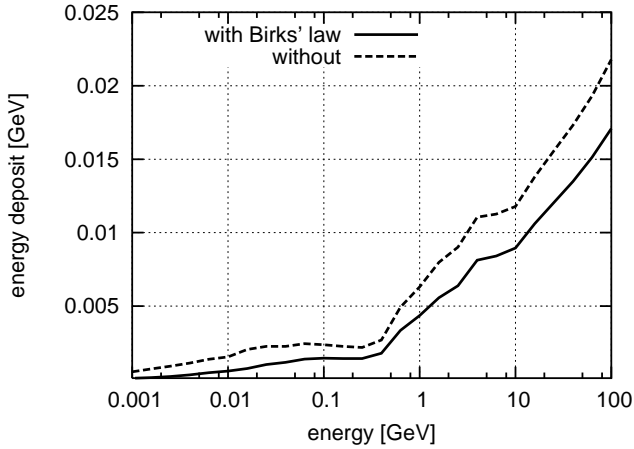


FIG. 6: The effect of Birks' law on the effective energy deposition spectrum of neutrons.

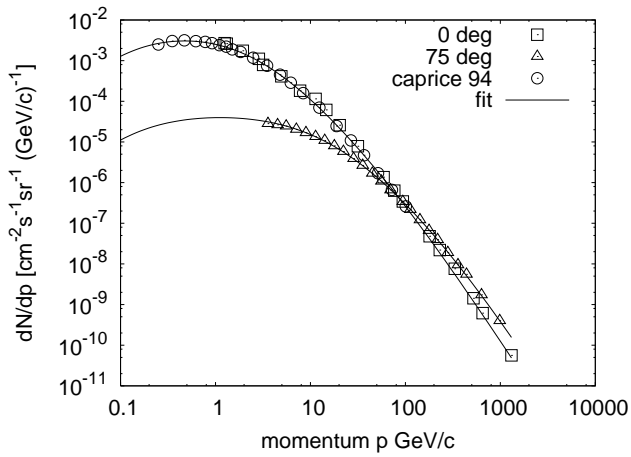


FIG. 7: The fitted distributions of atmospheric muons.

From data of refs. [15, 16] and Caprice 94 data [17], a functional fit of the muon spectrum $dD(p, \theta)/dp$ is obtained; data and fit are shown in Fig. 7. Then a Monte Carlo simulation is performed, in which muons are produced with this distribution and propagated through our detector simulation. Here, it is crucial to apply a smearing function to the energy deposit to reproduce the experimental shape of the pulse width distribution. We have found that a suitable smearing function is $P(x) \sim \exp(-0.5 \ln^2(xb)/\sigma^2)/x$, which can be obtained by taking the exponential of a random number sampled from a Gaussian distribution around zero and with width σ . Empirically, this function imitates Landau fluctuations in the photo-multiplier tube. The parameter b is adjusted such that the mean is equal to one: $\int xP(x)dx / \int P(x)dx = 1$. The values $\sigma = 0.3$ and $b = 1.045$ proved to describe best the shape of the PWD observed by AGASA. The quality of this fit is shown in

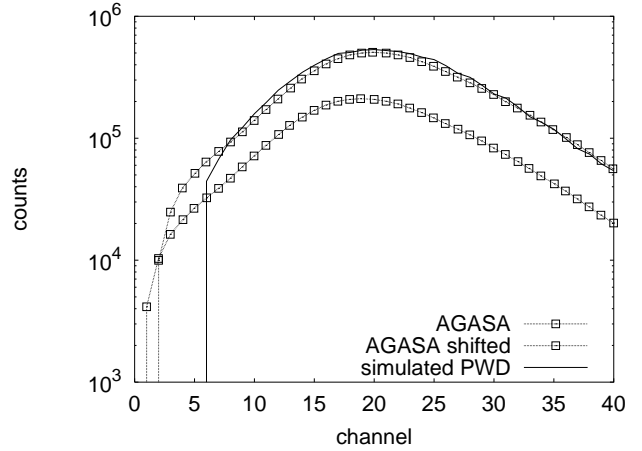


FIG. 8: Theory calibration according to the experiment. Each channel corresponds to 500ns. AGASA calibrates with the peak value t_1 whereas we calibrate the threshold of the signal (energy deposit) such that the peak is at $t_1 = 10\mu s$.

Fig. 8.

The next step in calibration is to set the absolute normalization of the signal. To convert AGASA's calibration to an energy scale we need to return to a more detailed discussion of their data recording procedure, which was described schematically in section III. If the signal threshold is set at V_{thr} , then the time-above-threshold or pulse-width, t_P , is implicitly given by [1]

$$V_{\text{thr}} = V \exp(-t_P/\tau), \quad (2)$$

where V is the pulse-height of the signal, proportional to the scintillation response and therefore to energy deposit. A priori, V and V_{thr} are measured in an arbitrary unit relating to the gain of the PMTs.

By defining t_1 as the pulse-width of a single particle with pulse-height V_1 one obtains

$$V_{\text{thr}} = V_1 \exp(-t_1/\tau), \quad (3)$$

and

$$N = \frac{V}{V_1} = \exp((t_P - t_1)/\tau) \quad (4)$$

as the number of particles for a arbitrary pulse-width t_P . One can consider N as some effective number of particles, since it comprises different particle types. AGASA sets their gain and threshold so that the peak of the pulse-width distribution of atmospheric muons occurs roughly in channel 20, as shown in Fig. 8. This corresponds to $t_1 \approx \tau = 10\mu s$ because one channel is 500ns. The precise calibration is then given by the peak value t_1 .

In our case the signal is just the energy deposit E in the plastic scintillator, so $V \rightarrow E$ applies to all formulas above. We calibrate the threshold E_{thr} such that the peak of the pulse-width distribution of omnidirectional

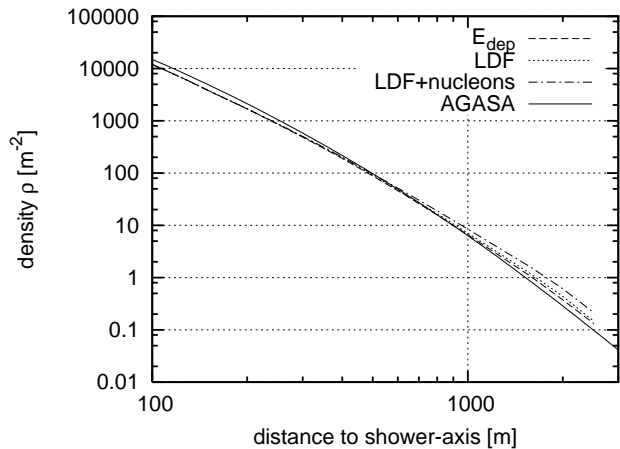


FIG. 9: LDF for a 10^{19} eV vertical proton induced shower using QGSJET01/GHEISHA.

muons is exactly at $t_1 = \tau = 10\mu\text{s}$. According to (3), the energy deposit of an effective particle is then $E_1 = E_{\text{thr}}/\exp(-1)$ and for arbitrary t_P the effective number of particles is just

$$N = \exp(t_P/\tau - 1). \quad (5)$$

Our simulation shows that the peak in the energy deposition of the omnidirectional muons corresponds to $E_1 = 0.011$ GeV per particle.

VI. LATERAL DISTRIBUTION FUNCTIONS

The AGASA collaboration finds experimentally that the lateral distribution of particle density (as defined via equation (4)) can be described by the empirical function:

$$S(R) = C \left(\frac{R}{R_M} \right)^{-\alpha} \left(1 + \frac{R}{R_M} \right)^{-(\eta-\alpha)} \left(1 + \left(\frac{R}{1\text{km}} \right)^2 \right)^{-\delta}, \quad (6)$$

where the parameters $\alpha = 1.2$ and $\delta = 0.6$ are fixed, $R_M = 91.6\text{m}$ is the Moliere radius two radiation lengths above the altitude of the Akeno observatory, and the slope η at distances large compared to R_M is an experimentally determined function of the shower zenith angle θ : $\eta = 3.84 - 2.15(\sec\theta - 1)$ [1].

By fitting “data” from their Monte Carlo shower and detector simulation to the lateral dependence of equation (6), AGASA obtained the conversion formula (formula (1) from Ref.[1])

$$E = 2.03 \times 10^{17} S(600\text{m}) \text{eV}, \quad (7)$$

using calculations for the Akeno observatory at the altitude 900 m. It was realized later that the average altitude of the whole AGASA array is actually 667 m, significantly different from that of the Akeno sector only. However

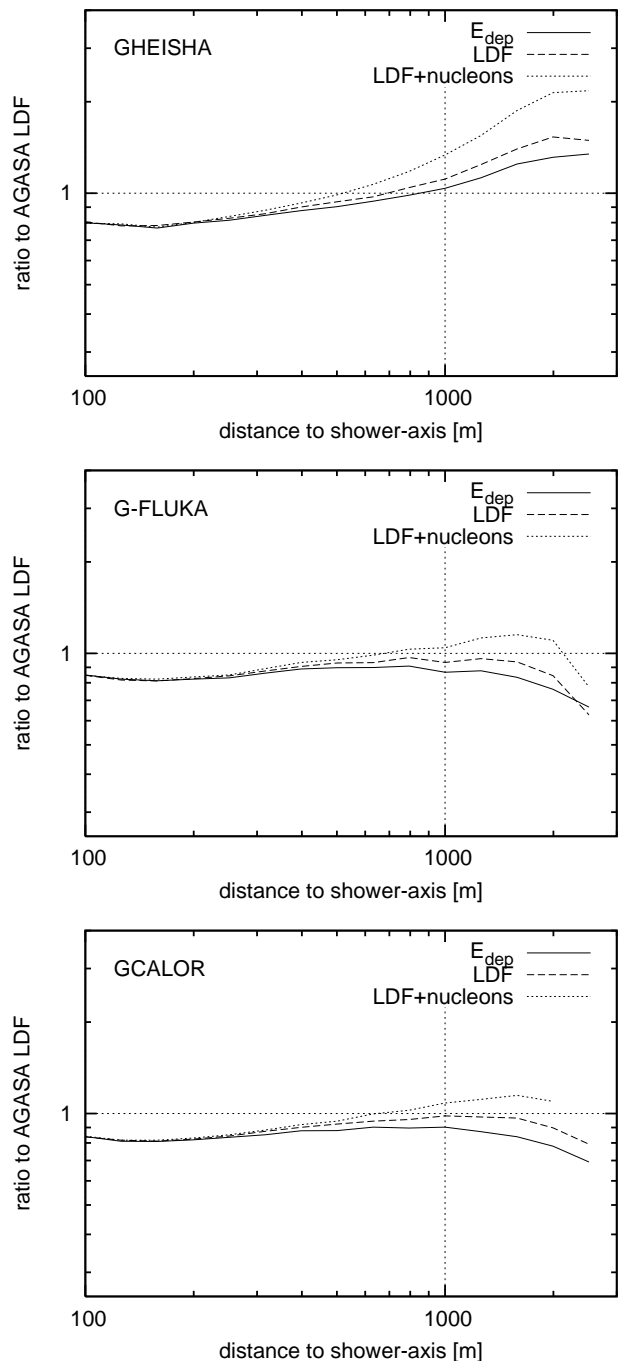


FIG. 10: LDF scaled by the AGASA empirical function for different low energy models and with the effects of the shower front and late nucleons.

when the AGASA analysis is corrected for the change in average altitude and still other effects (mainly shower front thickness and delayed particles – see table 2 from [1]), AGASA finds a final conversion formula which is coincidentally the same as their original one, (7). Below, when we refer to the AGASA LDF, we mean equation (6) normalized by (7).

We now compare the results of our calculations for various cases, to AGASA’s empirical results. We use an average altitude 667 m and the procedure of Sec. V to obtain the signal as a function of the energy deposit. Fig. 9 shows our predicted LDF for an average 10^{19} eV proton-induced vertical shower compared to the the AGASA empirical function (6). To quantify the importance of including the shower-front thickness and the contribution of nucleons, the figure shows three cases, all using QGSJET01/GHEISHA as the hadronic models. The curves are labeled E_{dep} , LDF and LDF+nucleons, and are computed as follows:

- E_{dep} : Only the energy deposit of electrons/positrons, muons, and photons is included; particles are assumed to arrive simultaneously.
- LDF: Same particles contributing as above, but with non-trivial distribution of shower front thickness taken into account.
- LDF+nucleons: the above, and additionally the effect of nucleons and their time delay taken into account.

One observes that the combination of hadronic models QGSJET01/GHEISHA, gives a slightly too flat slope of the LDF in all cases. This has already been found in ref. [18] based on “ E_{dep} ” alone. We see here that including the shower front thickness and the nucleons increases the discrepancy. This can be seen better in Fig. 10 where the results are shown as a ratio to the AGASA LDF. The lower panels of this figure show the LDF as obtained by choosing G-FLUKA and GCALOR as low energy hadronic model instead of GHEISHA. One sees that these two give a better description of the AGASA LDF, though still dropping slightly more slowly with distance. That the tails of LDFs can be sensitive to the low energy hadronic model has already been shown in ref. [19, 20, 21].

The values of the scaled LDFs at 600 m in Fig. 10 allow us to infer the deviation of AGASA’s energy estimation equation (7) from that implied by our simulations. Table I shows the ratio of our predicted signal to that “predicted” by AGASA using (7) as conversion factor, with QGSJET01 for the high energy model in each case. Thus for a given observed signal, if GHEISHA were the correct low-energy hadronic model AGASA would overestimate the energy of a vertical proton by about 5%, while if G-FLUKA or GCALOR correctly describe the low energy interactions, the AGASA energy estimate would be about 2% too low, when all the effects of late-arrivers and shower-front thickness are included.

VII. COMPARISON OF PREDICTED AND OBSERVED ARRIVAL TIME DISTRIBUTIONS

As discussed in Sec. II, given AGASA’s method of recording the signal, late arriving particles such as nu-

Model	deviation from (7)
QGSJET01/GHEISHA	1.049
QGSJET01/G-FLUKA	0.983
QGSJET01/GCALOR	0.978

TABLE I: The deviation of the energy estimation obtained in these simulations.

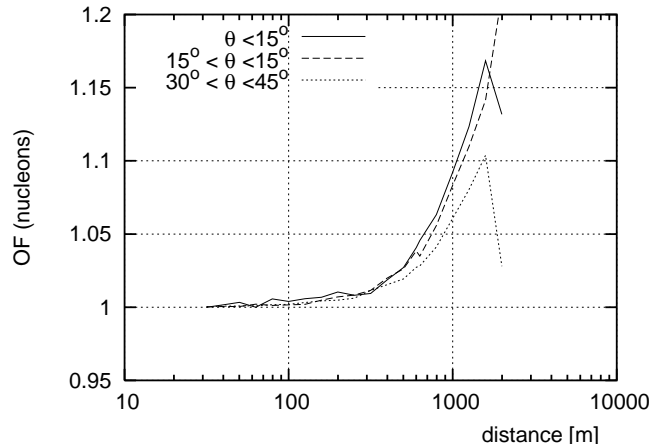


FIG. 11: Over-estimation factor due to late arriving nucleons as a function of radius, for 10^{19} eV proton-induced showers.

cleons could in principle distort the determination of the primary energy; Fig. 11 shows the simulated value of the overestimation factor f due to late arriving nucleons as a function of distance to the core. However as we saw in the previous section, the impact of late arrivers is compensated by other effects which had originally been neglected in AGASA’s calculations, so that we find the average AGASA energy determination to be quite good, assuming the primaries are protons and QGSJET01 is an adequate high energy model. The overestimation factor at 600m is not more than 5% for a vertical 10^{19} eV protons and we have confirmed it is the same for 5×10^{19} eV primaries.

The arrival time distribution itself has not up to now been critically compared to observations, which we do in this section. In addition to the standard detectors, the AGASA collaboration[1] used a $30 m^2$ detector in combination with the rest of the AGASA array to record the actual signal in that detector as a function of time, within $\pm 30 \mu s$ of the first particles of the shower. Ref. [1] remarked that including nucleons in model calculations gives an LDF which is much too flat compared to what is observed experimentally. We have found that this behavior can be produced by an imprecise implementation of energy loss.

The Bethe Bloch formula for the energy loss of charged particles diverges for values of the relativistic gamma-factor approaching $\gamma = 1$. When particles are propagated over a large distance in a single step, this divergence in dE/dx is not properly taken into account if the simula-

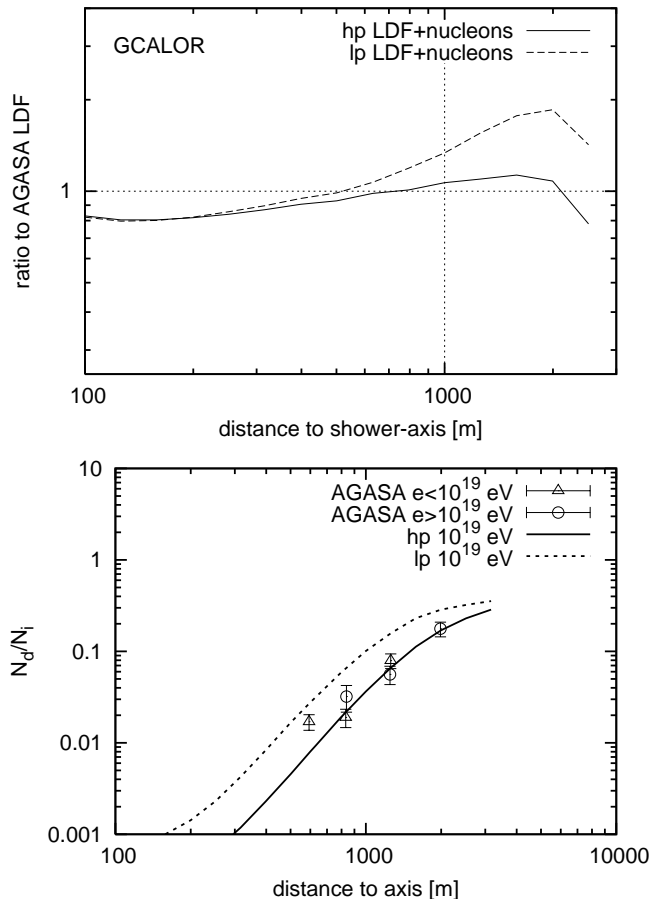


FIG. 12: LDF (upper panel) and fraction of delayed particles (lower panel) with high precision (hp) and low precision (lp) calculations of energy loss of charged particles.

tion calculates dE/dx at the starting point only and takes it to be the same over the total step length. If one takes for the step length the distance to the next interaction or decay, it is for non-relativistic particles often much too long for constant dE/dx to be a good approximation. For this reason the energy loss of protons, and neutrons coming from them as secondaries in the shower, is underestimated. A simple cure for this problem is to limit the step length to a suitably low value l_{\max} . We found that for $l_{\max} \leq 10$ m the results are stable, i.e., the low energy spectra of hadrons do not change any more as l_{\max} is reduced further.

The influence of the higher precision achieved can be seen in the upper panel of Fig. 12 where the LDF, including nucleons, has been calculated with high- and low-precision energy loss. “Low-precision” means taking the step length as proposed by the total cross-section of the interaction, usually several hundred meters at ground level, as done in standard simulations. It can be seen that the low precision energy loss calculation results in a significant overestimation of the LDF at large distances.

The change in precision is not important for particles

other than nucleons. Energy loss is accurately treated in electromagnetic shower codes, and when other charged particles such as muons and pions in the shower become non-relativistic they decay too quickly for their subsequent energy loss to matter. All results shown in this paper have been computed with high precision, for all charged particles in the shower.

Now we compare the observed delay time to our simulations. The lower panel of Fig. 12 shows the fraction of delayed particles as a function of the distance from the shower-axis, calculated with high and low precision. The data is from the AGASA collaboration measurement discussed above[1] and includes isotropically distributed showers up to 45° incident angle. The simulations are done in the same way, assuming purely proton primaries. The fraction of delayed particles is defined as the energy deposit of particles arriving later than $3 \mu\text{s}$ after the first particles in the detector, divided by the energy deposit of all particles. The late arrivers in the high precision calculation are reduced by a factor of two, and the results are in good agreement with the data.

VIII. SUMMARY AND CONCLUSIONS

We have analyzed the effect of late arriving particles on the energy determination of the AGASA experiment. We find that the net effect of the arrival time spread in the electromagnetic and muonic components of the shower, and the inclusion of nucleons in the simulation, has only a small effect on the AGASA energy determination. It shifts the true energy compared to the energy as determined without these effects, upward by a few percent in the models which give the best agreement with the shape of the lateral distribution function. This agrees with the correction applied by AGASA[1]. The LDF measured by AGASA is best described with G-FLUKA or GCALOR as the low energy hadronic model; the corresponding LDF using the GHEISHA code is too flat.

We have demonstrated for the first time that shower simulations can describe the distribution of arrival times of late-arriving particles, primarily nucleons, as observed by the AGASA collaboration[1]. When analyzing neutrons and protons in air shower simulations, the energy loss of charged particles has to be done with care. It is straightforward but crucial to compute these energy losses accurately, otherwise the contribution of these particles to the signal can be greatly overestimated. The Pierre Auger Observatory records detailed arrival time information in each tank, so accurately modeling the observed arrival time distributions should be a powerful new tool for validating shower simulations. An interesting question, left to the future, is to what extent the arrival time distribution can be useful for studying the composition of UHE cosmic rays.

Acknowledgments

HJD acknowledges support from NASA grant NAG 9246, and from the German BMBF/DESY grant 05CT2RFA/7; GRF is supported by NASA grant NAG-9246 and NSF-PHY-0101738.

Computations were done on computer clusters at NYU financed in part by the Major Research Instrumentation

grant NSF-PHY-0116590 and at the Center for Scientific Computing, Frankfurt am Main.

This research would not have been possible without M. Teshima's willingness to explain details of the AGASA detector and its signal processing procedures. We have also benefited from discussions with and assistance from many other colleagues including R. Djilbikaev, J. Sculli, A. Watson, S. Westerhoff, and Rex Tayloe.

-
- [1] M. Takeda et al. *Astropart. Phys.*, 19:447, 2003.
 - [2] T. Abu-Zayyad et al. *astro-ph/0208243*, 2002.
 - [3] H.J. Drescher and G.R. Farrar. *Phys. Rev.*, D67:116001, 2003.
 - [4] N.N. Kalmykov, S.S. Ostapchenko, and A.I. Pavlov. *Nucl. Phys. B (Proc. Suppl.)*, 52:17, 1997.
 - [5] W. R. Nelson et al. SLAC-265, Stanford Linear Accelerator Center, 1985.
 - [6] H. Fesefeldt. *PITHA 85/02, RWTH Aachen*, 1985.
 - [7] A. Fasso et al. In *Proceedings of the Workshop on Simulating Accelerator Radiation Environments*, page 134. Los Alamos Report LA-12835-C, 1992.
 - [8] T.A.Gabriel et al. *ORNL/TM-11185*.
 - [9] R. Brun, F. Bruyant, M. Maire, A. C. McPherson, and P. Zancarini. *CERN DD/EE/84-1*, 1987.
 - [10] G. Bossard et al. *Phys. Rev.*, D63:054030, 2001.
 - [11] D. Heck et al. *Report FZKA 6019*, 1998.
 - [12] N.Sakaki for the AGASA Collaboration. In *Proceedings of the 27th International Cosmic Ray Conference*, Hamburg, Aug. 7-15 2001.
 - [13] J. B. Birks. chapter 10.4.1. The Macmillan Company, 1964.
 - [14] J. B. Birks. chapter 6.1.2. The Macmillan Company, 1964.
 - [15] O. C. Allkofer, K. Carstensen, and D. W. Dau. *Phys. Lett.*, B36:425, 1971.
 - [16] H. Jokisch, K. Carstensen, W. D. Dau, H. J. Meyer, and O. C. Allkofer. *Phys. Rev.*, D19:1368, 1979.
 - [17] J. Kremer et al. *Phys. Rev. Lett.*, 83:4241, 1999.
 - [18] M. Nagano, D. Heck, K. Shinozaki, N. Inoue, and J. Knapp. *Astropart. Phys.*, 13:277, 2000.
 - [19] H.J. Drescher and G.R. Farrar. *Astropart. Phys.*, 19:235, 2003.
 - [20] H.J. Drescher et al. *Astropart. Phys.*, 21:87-94, 2004.
 - [21] H.J. Drescher et al. In *Proceedings of the 28th International Cosmic Ray Conference*, page 507, Tsukuba, Jul. 31-Aug. 7 2003.